

Review

Atmospheric Particle Number Concentrations and New Particle Formation over the Southern Ocean and Antarctica: A Critical Review

Jiayu Wang ¹, Guojie Xu ^{1,*} , Liqi Chen ² and Kui Chen ³ 

¹ Key Laboratory for Aerosol-Cloud-Precipitation of China Meteorological Administration, Nanjing University of Information Science and Technology, Nanjing 210044, China

² Polar and Marine Research Institute, College of Harbor and Coastal Engineering, Jimei University, Xiamen 361021, China

³ Emergency Management School, Nanjing University of Information Science and Technology, Nanjing 210044, China

* Correspondence: guojiexu@nuist.edu.cn; Tel.: +86-13236519328

Abstract: The Southern Ocean (SO) and Antarctica play important roles in the global climate. The new particle formation (NPF) alters the availability of cloud condensation nuclei (CCN), leading to impacts on the cloud reflectance and global radiative budget. In this review, we introduce the common instruments for measuring particle number concentration (PNC) and particle number size distribution (PNSD). Based on the observations over the Antarctic and some Antarctic research stations, we explored spatial and temporal characteristics of PNCs and PNSDs. From the SO to the interior of the Antarctic, the total PNCs show a decreasing trend, and the total PNCs present an obvious seasonal cycle, with the low concentration in winter (June–August) and the high concentration in summer (December–February). By summarizing the research progress over the SO and Antarctica, we discuss possible precursors of the NPF: sulfuric acid (H₂SO₄, SA), methanesulfonic acid (CH₃S(O)₂OH, MSA), dimethyl sulfide ((CH₃)₂S, DMS), iodic acid (HIO₃, IA), iodous acid (HIO₂), ammonia (NH₃), dimethylamine ((CH₃)₂NH, DMA), highly oxygenated organic molecules (HOMs) and other organics with low vapor pressure. We also explore several possible nucleation mechanisms: ion-induced nucleation of H₂SO₄ and NH₃, H₂SO₄-amines, H₂SO₄-DMA-H₂O, H₂SO₄-MSA-DMA, IA-MSA, IA-DMA, heterogeneous IA-organics nucleation mechanisms and environmental conditions required for the NPF. NPF is one of the main sources of CCN in the remote marine boundary layer, such as the SO and Antarctica. Thus, we discuss the contribution of NPF to CCN and the indirect impacts of NPF on climate. Through this review, we could better understand the PNC and NPF over the SO and Antarctica and their impacts on the global climate.

Keywords: Southern Ocean; Antarctica; number concentration; size distribution; new particle formation



Citation: Wang, J.; Xu, G.; Chen, L.; Chen, K. Atmospheric Particle Number Concentrations and New Particle Formation over the Southern Ocean and Antarctica: A Critical Review. *Atmosphere* **2023**, *14*, 402. <https://doi.org/10.3390/atmos14020402>

Academic Editor: Marco Paglione

Received: 17 January 2023

Revised: 15 February 2023

Accepted: 17 February 2023

Published: 19 February 2023



Copyright: © 2023 by the authors. Licensee MDPI, Basel, Switzerland. This article is an open access article distributed under the terms and conditions of the Creative Commons Attribution (CC BY) license (<https://creativecommons.org/licenses/by/4.0/>).

1. Introduction

The Antarctic atmosphere contains fewer aerosol mass and number concentrations [1]. Accordingly, natural emissions account for a significant proportion of the aerosol population, with sea spray and NPF from marine emissions likely to be the two major sources of aerosols. Other minor sources include volcanic emissions, emissions associated with seabirds and other animals, and windblown snow from ice-covered regions [2,3]. It is true that some emissions from research stations associated with transportation are attributed to local anthropogenic sources [4,5]. Since the 1990s, NPF events have been observed in forested areas [6], over rural continental areas [7,8], in various urban areas [9,10], and in the marine boundary layer [11,12]. The SO and Antarctic region is one of the few places left on our planet with conditions similar to the preindustrial age [13]. This provides an ideal environment for studying background conditions and processes associated with NPF [14].

There is little interference from land in the SO, which is a biologically active region emitting marine vapor precursors [15,16]. Over the Antarctic continent, aerosol particles almost entirely come from the surrounding marine areas [2]. Existing studies have shown that few NPF events occurred over the SO, while most of the NPF events occurred on the coast of Antarctica [17,18].

NPF is one of the major sources of atmospheric particles [19]. NPF is a process in which low-volatility vapors emitted from biological or anthropogenic sources condenses to form molecular clusters and then grow into larger particles through condensation or collisions [20,21]. The phenomenon is characterized by the sudden eruption of high concentrations of sub-nanometer particles (1–3 nm) in the atmosphere, followed by their continued growth [22]. Nucleation rate (J) or formation rate (FR) and growth rate (GR) are the key parameters used to characterize this phenomenon [23]. There is a significant impact of NPFs on regional and global climate, air quality, and human health [20]. Newly formed particles can then grow to a size large enough to act as CCNs, affecting the physical properties of cloud droplets and indirectly affecting the Earth's radiation balance and global climate. Limited understanding of the mechanism of NPF is existed, especially over the remote oceanic regions. As a result, there are significant uncertainties in the model simulations, which will directly affect the prediction of climate change effects [24].

PNSD is one of the important parameters to judge whether an NPF event has occurred [20]. In atmospheric environments, the PNSD is mainly on four modes: the nucleation mode ($D_p < 30$ nm), the Aitken mode ($30 \text{ nm} < D_p < 100$ nm), the accumulation mode ($100 \text{ nm} < D_p < 1 \mu\text{m}$) and the coarse mode ($D_p > 1 \mu\text{m}$) [25]. In practice, NPF event identification is performed visually by classifying the NPF event or non-event days from the PNSD surface plots [26]. In NPF events, the PNSD is characterized by an explosive increase in number concentration in the nucleation mode, and the particles continue to grow to larger sizes [20].

Atmospheric NPF is proposed to be a two-step process. The first step would be the nucleation process itself, which produces atmospheric clusters (neutral or ionic). The second step would be the activation of clusters [27]. General gaseous precursors for nucleation include SA, MSA, IA, HIO_2 , oxalic acid (OxA), NH_3 , DMS, methylamine (MA), DMA, HOMs, and other organics [28–30]. A number of organic acids such as formic, acetic, pyruvic acids and OxA have been found to contribute to the initiation of nucleation in polluted urban air and they are lower in the remote marine atmosphere [31,32].

The current nucleation mechanisms include the homogeneous homomolecular nucleation (HHN) (e.g., the nucleation of pure water), the binary homogeneous nucleation (BHN) (e.g., $\text{H}_2\text{SO}_4\text{-H}_2\text{O}$ binary system), the ternary homogeneous nucleation (THN) (e.g., OxA-MA-MSA ternary system), the ion-induced nucleation (IIN) (e.g., ion-induced nucleation of $\text{H}_2\text{SO}_4\text{-H}_2\text{O}$ or ternary inorganic vapors or of organic vapors), and barrier-less (kinetically controlled) homogeneous nucleation of, for example, iodide species [27,33,34]. BHN mainly occurs in the free troposphere and in the stratosphere. In most cases, THN occurs in the boundary layer [27,35]. It is primarily found in the upper troposphere and the lower stratosphere, where IIN occurs. On average, the IIN in the boundary layer seems to be mostly around or below 10% of particle formation [36,37]. Barrier-less homogeneous nucleation of iodide species mainly occurs in the coastal environment [27,37]. The upper troposphere is well recognized as a region of particle formation [38]. In the troposphere, ion-mediated $\text{H}_2\text{SO}_4\text{-H}_2\text{O}$ nucleation appears to dominate over neutral $\text{H}_2\text{SO}_4\text{-H}_2\text{O}$ nucleation, both in the lower as well as middle and upper troposphere. There is evidence that binary nucleation of $\text{H}_2\text{SO}_4\text{-H}_2\text{O}$ and ternary nucleation of NH_3 are the dominant processes responsible for NPF in the middle and upper troposphere [30,39]. In the remote ocean, there may be $\text{H}_2\text{SO}_4\text{-H}_2\text{O}$, $\text{H}_2\text{SO}_4\text{-NH}_3\text{-H}_2\text{O}$, $\text{H}_2\text{SO}_4\text{-DMA}$, $\text{H}_2\text{SO}_4\text{-DMA-H}_2\text{O}$, $\text{H}_2\text{SO}_4\text{-MSA-DMA}$, ion-induced nucleation of H_2SO_4 and NH_3 , IA-MSA, IA-DMA, the heterogeneous processes of iodine with organics and other nucleation systems [12,31,32,40,41]. Additionally, the initial steps of aerosol growth can take place via several ways: 1. condensation of nucleating vapors; 2. charge-enhanced condensation; 3. self-coagulation; 4. multi-phase chemical

reactions; 5. cluster activation by heterogeneous nucleation; 6. cluster activation by soluble vapors. The first three mechanisms do not require any help from vapors other than those participating in the nucleation process, whereas the last three mechanisms need some additional vapors, such as organic vapors, to participate in the growth process [27].

Although the environment in the SO and Antarctica is harsh and it is difficult to conduct field observations, lots of studies have focused on the atmospheric PNC and NPF. In this review, we summarize the method and instruments utilized to measure atmospheric PNC. Spatial and seasonal variations of atmospheric PNC and PNSD over the SO and Antarctica are also reviewed. Lastly, we discuss precursors of nucleating, nucleation mechanism, environmental influencing factors and contribution of NPF to CCN over the SO and Antarctica. A detailed understanding of the PNC, NPF and their subsequent growth over remote oceanic regions will improve our understanding of the formation process of atmospheric aerosols.

2. Instrumentation

The main measurement parameters for studying NPF include the concentration of gaseous precursors of new particles, the number size distributions of nanoparticles or positive and negative ions, the chemical composition of ultrafine particles, as well as the moisture absorption and volatility of particles [24]. It is necessary to measure PNC and PNSD at nanometer levels in order to identify NPF events and retrieve parameters that describe particle formation processes, such as formation and growth rates [22]. What is more, the phase change between vapor and liquid typically appears at around 1–2 nm in diameter. The size difference between molecules, clusters, and particles (about 1–3 nm) poses a challenge for both theory and experiments. In recent years, since great progress has been made in developing optimized instruments for measuring the smallest size particles, the minimum particle size that can be measured by commercial instrument has reached 1 nm [22,27,37]. As shown in Table 1, there are many instruments that can be used to measure PNC and PNSD, including air ion spectrometer (AIS), condensation particle counter (CPC), differential mobility particle sizer (DMPS), particle size magnifier (PSM) and aerodynamic particle sizer (APS). The common instruments used over the SO and Antarctica include the CPC, DMPS, AIS, etc.

Table 1. Parameters of instrument for measuring PNC.

Instrument	Manufacturing Company	Principle	Size Range (nm)	Reference
AIS	Airel	electrical mobility size	0.46–55	[27]
CPC 3007	TSI	aerodynamic size	10–1000	[42]
DMPS	GRIMM	electrical mobility size	10–800	[43]
PSM	Airmodus	aerodynamic size	<1	[42]
APS	TSI	optical size	500–20,000	[44]

A CPC, also known as a condensation nucleus counter (CNC), is used to measure atmospheric PNC. Its basic principle involves the flow of sampled aerosol over a warm reservoir of a working fluid, where it becomes saturated with a condensable vapor. The vapor becomes supersaturated during subsequent cooling to a condensed state, allowing particles to grow into large liquid droplets of 10 μm in diameter, which can be detected individually by light scattering. The CPC 3007 is able to measure particle sizes ranging from 0.01 μm to 1.0 μm , with a concentration range of 0–100,000 particles cm^{-3} . There is a detection range of 0.02 μm to greater than 1.0 μm and a maximum concentration of 500,000 particles cm^{-3} [42]. For the generation of particle size spectra, the CPC may be connected to a particle size spectrometer, such as DMPS/SMPS [24].

The DMPS is an instrument for online sizing gas-borne particles in spectrometer and nanometer diameter ranges [45]. It is typically composed of a differential mobility analyzer (DMA) that electrostatically classifies particles with diameters between a few nanometers and a micrometer, as well as a CPC that measures the concentration of size-

selected aerosol particles [46]. By flowing the aerosol through an annular gap between two coaxial cylindrical electrodes, the DMA classifies particles based on their electrical mobility [47]. Clearly, the DMA is one of the most effective instruments for measuring aerosol particles with diameters ranging from nanometers to almost microns [48]. The DMPS system measures the PNSD between 10 and 800 nm, with some ultrafine systems extending down to 3 nm [44]. DMPS is capable of achieving high sampling rates and efficient separation between the Aitken and accumulation modes due to its high particle size resolution as compared to earlier instruments [49].

The AIS measures mobility and PNSD of atmospheric ions. The neutral cluster and air ion spectrometer (NAIS) can additionally measure neutral particles. The NAIS is able to measure neutral clusters down to 1.2–1.5 nm. AIS is capable of measuring the mobility distribution of air ions (naturally charged clusters and aerosol particles) in the range of $0.00075\text{--}2.4\text{ cm}^2\text{ V}^{-1}\text{ s}^{-1}$, and the corresponding diameter ranges for single charged particles are 0.46–55 nm [27]. Large flow rates are often used in ion spectrometers in order to reduce particle losses; however, the noise associated with large flow rates can pose a problem at low particle concentrations [22].

Last but not least, the traditional atmospheric sensors utilized for chemical analysis and PNSD measurement normally are very expensive and labor-intensive in operation and troubleshooting [22]. Newly developed low-cost, portable and reliable instruments have been utilized to provide detailed size information about clusters and nanoparticles [50].

3. Progress on Research of Atmospheric PNCs over the SO and Antarctica

3.1. Spatial Variation

PNCs and PNSDs over the SO differ from those over the tropics, northern mid-latitude oceans, and the Arctic Ocean. The results of a research cruise from the English Channel to the coast of Antarctica show that no nucleation mode has been found in the marine air mass measured north of 40°S , indicating that the nucleation mode is extremely rare in the tropical and northern mid-latitude pristine ocean air. When approaching the Antarctic, the nucleation mode started to occur more frequently with peak concentrations close to $1000\text{ nuclei cm}^{-3}$ [18]. As a result of the Antarctic Circumnavigation Expedition: Study of Preindustrial-like Aerosols and Their Climate Effects (ACE-SPACE) over the SO, it has been demonstrated that the total concentration of PNCs varied between 10 and $>1000\text{ cm}^{-3}$, while the summer Arctic Ocean concentration spanned a greater range of 1 to $<4000\text{ cm}^{-3}$ during the Arctic Ocean 2018 expedition [51]. It can be concluded that the nucleation mode of the SO is more common than that of tropical and northern mid-latitude oceans, and the total aerosol number concentration over the SO is lower than that over the Arctic Ocean.

An obvious spatial variation can be observed between the Antarctic coast and the inland in terms of total PNCs and PNSDs. PNC distributions over the SO and Antarctica are shown in Figure 1. During the austral summer between 2000 and 2001, total PNCs and PNSDs within a diameter range of 3 to 800 nm were measured in continental Antarctica at the Finnish Antarctic station Aboa ($73^\circ03'\text{ S}$, $13^\circ25'\text{ W}$). The total number of PNCs observed varied between 200 and 2000 cm^{-3} . Concentrations in excess of about $300\text{--}400\text{ cm}^{-3}$ were attributable to the presence of small ($<20\text{ nm}$) nucleation mode particles. The measured size distributions were fitted with two to four lognormal modes. All number size distributions displayed an Aitken mode, with the diameter peaking at about 30–50 nm, and an accumulation mode peaking at about 70–150 nm [52]. During the austral summer of 2006, PNSD measurements were performed in the 10–500 nm size ranges over the Nansen Ice Sheet glacier ($74^\circ30'\text{ S}$, $163^\circ27'\text{ E}$). A monomodal number size distribution, peaking at about 70 nm with no variation during the day, was observed associating with the continental air mass, high wind speed and low relative humidity. Trimodal number size distributions were also observed. In this case, NPF was observed with subsequent particle growth up to about 30 nm [48]. During two summer campaigns in January 2015 and January 2016, PNSDs were measured at the continental Antarctic station Kohnen ($75^\circ00'\text{ S}$, $00^\circ04'\text{ E}$). During the accidental impact of a unique low-pressure system in 2015, the physical and

chemical properties of aerosols were significantly different from those of generally clear skies. The occurrence of an NPF event exhibiting a continuous growth of D_p from 12 to 43 nm over 44 h (growth rate 0.6 nm h^{-1}). On the whole, aerosol deposition on-site during austral summer should be largely dominated by typical steady clear sky conditions. Under clear sky conditions, aged aerosol, characterized by usually mono-modal size distributions around $D_p = 60 \text{ nm}$, was observed [53]. A brief summary of some PNCs and PNSDs involved in the events described above can be found in Table 2.

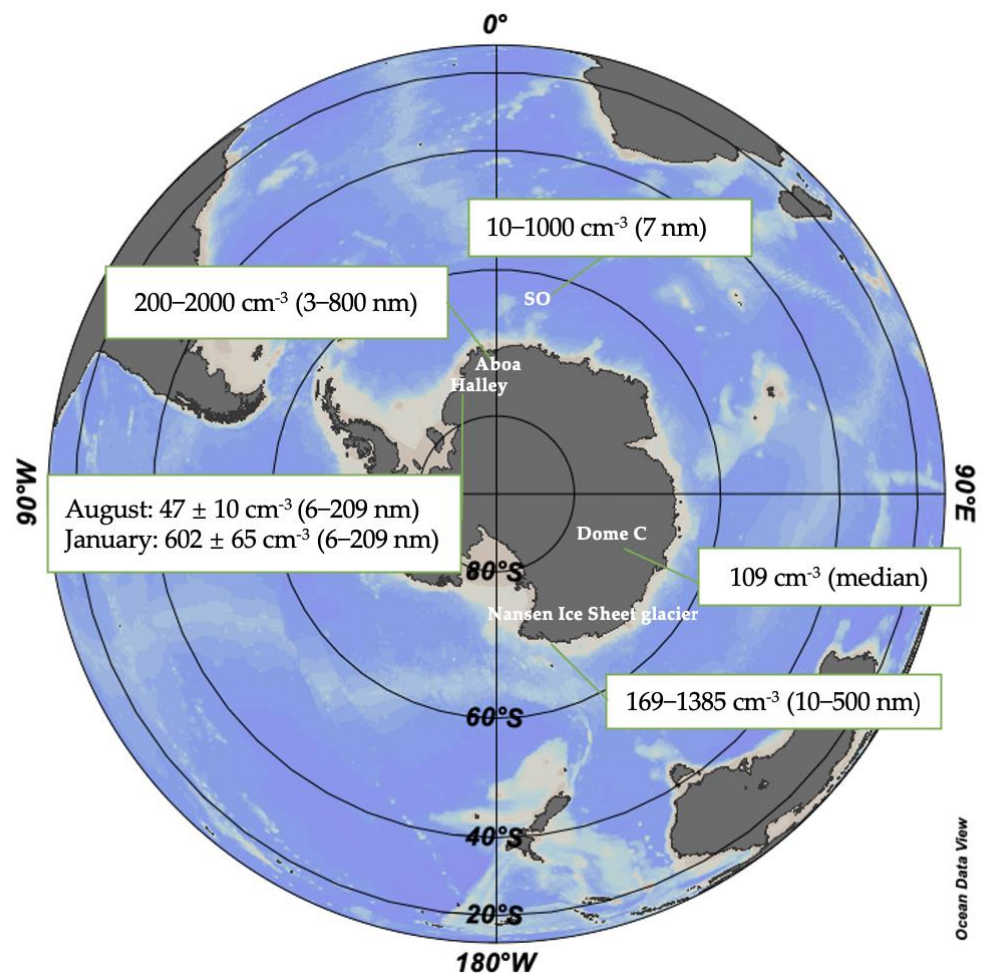


Figure 1. Total aerosol number concentrations over the SO and Antarctica.

Table 2. Key parameters and related meteorological elements of NPF events occurred over the SO and Antarctica.

Location	Lat. And Long.	Study Period	Wind Speed (m s ⁻¹)	Relative Humidity (%)	Total PNC (cm ⁻³)	FR (cm ⁻³ s ⁻¹)	GR (nm h ⁻¹)	Reference
The Finnish Antarctic station Aboa (Antarctica)	73°03' S, 13°25' W	January 2010	~	~	~	0.003–0.3 (J10)	~	[2]
The Marambio Station (Antarctic Peninsula)	64°15' S, 56°38' W	15 January 2018–25 February 2018	1–20	<75	~	0.69 (J3)	4.2 (3.8–12 nm)	[29]
Nansen Ice Sheet glacier (the Ross Sea)	74°30' S, 163°27' E	2006	1–5	>80	169–1385	~	4	[49]
The Finnish Antarctic station Aboa (Antarctica)	73°03' S, 13°25' W	5 January 2000–22 January 2000 and 1 January 2001–26 January 2001	~	40–100	200–2000	~	2 (3–15 nm)	[52]
The Concordia station (Dome C)	75°06' S, 123°23' E	14 December 2007–7 November 2009	~	~	109 (median)	~	2.5	[54]
The King Sejong Station (Antarctic Peninsula)	62°12' S, 58°48' W	May 2009–December 2016	~	~	1707–83,120	2.79 ± 1.05 (J2.5–10)	0.68 ± 0.27	[3]

3.2. Seasonal Variation

The Antarctic aerosol system exhibits an obvious annual cycle of total PNCs and PNSDs. The PNCs display the maximum value during the austral summer, and the minimum value during the austral winter. The coarse particles are enhanced during the winter-spring (June–November), while fine particles are enhanced during the summer [13,55,56]. A cluster analysis of the physical characteristics of PNSDs was conducted in the size range of 6–209 nm at Halley Station (75°36' S, 26°11' W) in the whole year of 2015. The lowest concentration in August was $47 \pm 10 \text{ cm}^{-3}$, and the maximum concentration in January was $602 \pm 65 \text{ cm}^{-3}$. In the annual average size distribution, an obvious peak was shown at 45 and at 145 nm. Nucleation and Aitken mode dominated in summer months (59–90%), whereas a clear bimodal size distribution (peaking at 43 and 134 nm) was seen during the December–April period (6–21%) [13]. From 14 December 2007 to 7 November 2009, PNSDs were measured in the size range 10–600 nm on the high East Antarctic plateau at the Concordia station, Dome C (75°06' S, 123°23' E). The total PNC was low with the median of 109 cm^{-3} . The concentrations were at their highest during the austral summer with the median values of 260 cm^{-3} , and at their lowest during the austral winter with corresponding values of 15 cm^{-3} [3]. Relevant results showed that seasonal features of PNC are associated with primary emissions of sea-salt aerosols, NPF, emissions of aerosol precursors from oceanic bioactivity, and photochemical processes [4]. Aerosol emissions from the surfaces of ocean and sea ice through wind blowing processes might cause aerosol enhancement in fine and coarse modes in the Antarctic coasts during winter-spring [55,56]. Simulations conducted by Yu et al. (2010) indicated that increases in DMS emission and photochemistry during the austral summer resulted in significant new particle formation through ion-mediated nucleation and significantly higher particle numbers over Antarctica and the surrounding oceans [57].

4. Progress on Research of NPF Evens over the SO and Antarctica

4.1. Precursors and Nucleation Mechanism

Over the SO and Antarctica, condensable vapors related to NPF and particle growth include SA, MSA, DMS, IA, HIO₂, NH₃, DMA, HOMs and other organics with low vapor pressure. On the other hand, nucleating ion clusters such as bisulfate ions with SA and NH₃ and bisulfate ions and neutral SA with DMA are previously identified as participating in aerosol formation processes [28,29,58,59]. The SO has high biological activity and is a source of numerous aerosol precursor vapors, including DMS, volatile organic compounds, molecular iodine, and iodine hydrocarbons [58]. It is estimated that sea surface DMS concentrations in the SO are the highest on the planet, reaching mean values of more than 5 nm during the austral spring-summer (September–February) season [60]. DMS is a biological compound produced by phytoplankton. SA and MSA are formed from the oxidation of DMS [61]. Although the chemical production of IA is not fully resolved, IA results from the oxidation of reactive iodine (in the form of I₂, HIO, or intermediate I) that is released from algae and phytoplankton emissions contained within the seawater, ice, and snow [29]. In addition, the sea ice area in the Antarctic Peninsula-western Weddell Sea region is the main source of amines. Sympagic waters in this region have been shown to be rich in methyl, dimethyl and trimethyl amines and their precursors [28]. Sources of ammonia over the SO are related to animals, mainly bird or seal colonies, which are known to be strong local sources of ammonia [61]. The primary sources of air ions are radon decay, gamma radiation, and cosmic radiation [62]. It has been reported that galactic cosmic rays are the sole source of ions in the Antarctic lower atmosphere, and they may play an important role in NPF in this region [58].

There is a high concentration of SA, MSA, and IA over the SO and Antarctica [40]. SA is the most important vapor for particle formation and initial growth [63]. The concentration of gaseous SA over $10^5 \text{ molecules cm}^{-3}$ is the necessary condition for the NPF [64]. SA is considered as the most prevalent nucleating species because of its low vapor pressure under typical atmospheric conditions. Moreover, SA is prone to form hydrogen bonding with

many atmospherically important compounds, including water, basic species (i.e., ammonia and amines), and organic acids [22]. There has been evidence that amines and ammonia can be important stabilizers for SA in the formation of particles in marine environments [65]. Ions can play a comparable role in stabilizing nucleating acidic or biogenic particles [66]. According to some observations on the Antarctic Peninsula, SA is an important contributor to NPF processes, while MSA and IA are likely to only contribute to particle growth [28,29]. In marine and polar environments, the iodine oxide and IA has a major contribution to the iodine nucleation process. However, the nucleation mechanism of iodine-containing substances over the SO and Antarctica is still uncertain [41].

It is evident from Table 3 that nucleation mechanisms over the Antarctic may include ion-induced nucleation of H_2SO_4 and NH_3 , H_2SO_4 -amines, H_2SO_4 -DMA- H_2O , H_2SO_4 -MSA-DMA, IA-MSA, IA-DMA and heterogeneous iodine-organic systems [12,28,29,41,58,67,68]. The ion-induced nucleation of H_2SO_4 and NH_3 is the predominant mechanism for growth and NPF in coastal eastern Antarctica, and possibly throughout the lower-troposphere coastal Antarctic region. Ions induce the nucleation of H_2SO_4 and NH_3 , and then H_2SO_4 drives the growth. The nucleation rates are likely to be highly sensitive to both H_2SO_4 and NH_3 . Therefore, any change in marine phytoplankton DMS production, volcanic activity, or biological ammonia sources may be rapidly reflected in the new particle and eventually CCN concentrations over the Southern Hemisphere [58]. Around the Antarctic Peninsula, the NPF is driven by H_2SO_4 and alkylamines. Alkylamines have been shown to enhance formation rates at modest mixing ratios in the range of a few parts per trillion by volume, which are sufficient to substitute NH_3 in H_2SO_4 - NH_3 clusters. [28]. In addition, it is possible that DMA nucleates efficiently with H_2SO_4 and may be primarily responsible for the formation pathway of the neutral new particle H_2SO_4 -DMA- H_2O . On the other side, MSA has been shown to accelerate the nucleation of H_2SO_4 and DMA, with which it forms stable clusters in the H_2SO_4 -MSA-DMA system [28,29]. Research has demonstrated that IA-MSA, IA-DMA and heterogeneous iodine-organic nucleation systems may exist in remote marine areas [12,41,68]. The MSA in IA-MSA systems is capable of stabilizing IA clusters by forming hydrogen and halogen bonds, thereby promoting IA cluster formation rate, particularly in low-temperature environments where IA is sparse and MSA is abundant [41]. In the case of the IA-DMA system, DMA can structurally stabilize IA via hydrogen and halogen bonds, and the clustering process is energy barrierless [68]. For heterogeneous IA-organics system, nucleated iodine oxide clusters provide unique sites for the accelerated growth of organic vapors to overcome the coagulation sink. Heterogeneous reactions form low-volatility organic acids and alkylammonium salts in the particle phase, while further oligomerization of small α -dicarbonyls (e.g., glyoxal) drives the particle growth [12]. In addition, considering previous observations in the Arctic and Antarctic environment, Sipilä et al. (2016) demonstrated iodine-related nucleation as successive addition of multiple IA and water groups, and it was unlikely that IA promotes nucleation through either neutral or ion-induced mechanisms at this Antarctic site [69]. According to the field studies [17,69], in the coastal Mace Head, Ireland, the observed intense NPF events happen during the low tide and are associated with a significant increase in iodic acid (HIO_3 , IA) concentration. This indicates that the coastal NPF is primarily controlled by the subsequential addition of IA, during which the participation of I_2O_5 is involved. However, there have been a limited number of studies conducted in the Antarctic region concerning iodide nucleation. In the future, more research on atmospheric iodide nucleation in the Antarctic region should be conducted [12,17,41,69,70].

Table 3. Summary of the reported NPF mechanisms over the SO and Antarctica.

Nucleation Mechanism	Region	Location	Reference
H ₂ SO ₄ -DMA-H ₂ O	Antarctic Peninsula	62°36' S, 60°30' W	[28]
H ₂ SO ₄ -MSA-DMA	Antarctic Peninsula	64°15' S, 56°38' W	[29]
H ₂ SO ₄ -DMA-H ₂ O	Antarctic Peninsula	64°15' S, 56°38' W	[29]
H ₂ SO ₄ -NH ₃ -H ₂ O	Coastal Antarctica	73°03' S, 13°25' W	[58]
OxA-MA-MSA	Polluted area	~	[30]
Iodine-organics	Coastal areas	53°20' N, 9°54' W	[12]
IA-MSA	Marine	~	[41]
IA-DMA	Marine	~	[41]

4.2. Environmental Influencing Factors

The NPF is affected by a number of factors. Photochemistry plays a key role in NPF, which is reflected in that most NPF events occur in the daytime [71,72]. Other features common to conditions favorable to NPF are low condensation sink (pre-existing aerosol concentration), low relative humidity, and high vapor source rate [37]. There is also evidence that aerosol formation is related to atmospheric mixing processes, such as the evolution of a continental boundary layer or the mixing of stratospheric and tropospheric air near the tropopause [27]. Over the SO and Antarctica, NPF events were observed during days with high solar radiation, mostly with above-freezing temperatures and with low relative humidity [29]. Temperature and condensation sink may be the reason why this process occurs more frequently along the coast of Antarctica than in the open Southern Ocean reported in many studies [61]. There is a high frequency of NPF events in austral summer (72%), while there is a low frequency in austral winter (38%). In summer, the maximum solar radiation can reach 800 W m⁻², and it is estimated that the midday OH concentration can be estimated to be 3.4 × 10⁶ molecules cm⁻³ [50,70]. The clear difference in austral summer and winter indicates that solar intensity and temperature play important roles in the formation and growth of aerosol particles [3].

There is a prevailing opinion that NPF rarely occurs in remote marine boundary layers over open oceans. However, there is a regular and frequent occurrence of NPF in the upper portion of the remote marine boundary layer following the passage of cold fronts. The NPF is facilitated by a combination of efficient removal of existing particles by precipitation, cold air temperatures, vertical transport of reactive gases from the ocean surface, and high actinic fluxes in a broken cloud field [11].

In addition to the environmental conditions discussed above, cloud has an impact on NPF as well. In the SO, cloud-based convective transport of air masses into the free troposphere has been shown to result in NPF. The colder air temperatures of the free troposphere promote partitioning into the aerosol phase, while the in-cloud wet scavenging of CCN removes competing condensation sinks. Depending on the precursor concentrations, when entrained back into the marine boundary layer in the cloud outflow regions, these newly formed aerosols can greatly increase nucleation or even Aitken mode aerosol number concentrations [15]. However, NPF events will also be reduced by the presence of clouds. Clouds reduce the probability of NPF occurring by attenuating the solar radiation intensity below the cloud layer. When clouds appear or a solar eclipse occurs, an ongoing NPF event can be interrupted [73].

Additionally, human activities may contribute to the formation and concentration of high levels of aerosols [3]. NPF will also be affected by anthropogenic activities in Antarctica (power generation, vehicles, ships and aircraft). The model results of Chen et al. (2021) suggest that anthropogenic organic species play an important role in the formation and growth of aerosol particles at polluted sites and worldwide [74]. The total annual SO₂ is 158 Mg from power generation and vehicle operations, 3873 Mg from ships and 56 Mg from aircraft for 2004–2005 in Antarctica [75]. Though these figures are small, comparing with emissions at most other world regions, they are an indication of local pollutions by human being activities in the Antarctic.

4.3. NPF Contribution to CCN

NPF is one of the main sources of global aerosol particles and CCN [76]. In particular, ultrafine particles of <100 nm in diameter can contribute to maximum CCN generations of 40% and 90% at the boundary layer and in the remote free troposphere [77]. Based on a global aerosol microphysics model, Merikanto et al. (2009) quantified the contribution of primary and nucleated particles to global CCN. The model showed 55% of CCN (0.2%) are from nucleation, with 45% entrained from the free troposphere and 10% nucleated directly in the marine boundary layer [78]. During the 2018 Southern Ocean Clouds, Radiation, Aerosol Transport Experimental Study (SOCRATES) aircraft campaign, findings indicated that the SO free troposphere (3–6 km) is characterized by widespread, frequent NPF events contributing to much larger concentrations ($\geq 1000 \text{ mg}^{-1}$) of condensation nuclei (diameters $>0.01 \mu\text{m}$) than in typical sub-tropical regions [79]. Over the SO, biogenic sulfur-based particles $>0.1 \mu\text{m}$ diameter contribute the majority of CCN number concentrations in summer [76].

NPF may prove to be a key tool for predicting the future climate of polar regions. The aerosol indirect radiative forcing is largely determined by the number abundance of particles that can act as CCN [36]. In the Indian Ocean sector of SO, the resultant clear sky direct shortwave radiative forcing was $1.32 \pm 0.11 \text{ W m}^{-2}$ [80]. On King George Island, direct aerosol radiative forcing was between -2 and 4 W m^{-2} [81]. Because of low aerosol number concentrations, direct effects of aerosol radiative forcing are negligible in the Antarctic [55]. As shown in Figure 2, NPF has an impact on the climate. The gas-phase formation of new particles less than 1 nm in size and their subsequent growth significantly alters the availability of CCN, leading to impacts on cloud reflectance and the global radiative budget [7]. The mechanism of NPF over the SO and Antarctica and its contribution to CCN require further research in order to accurately predict future climate change in polar regions [76].

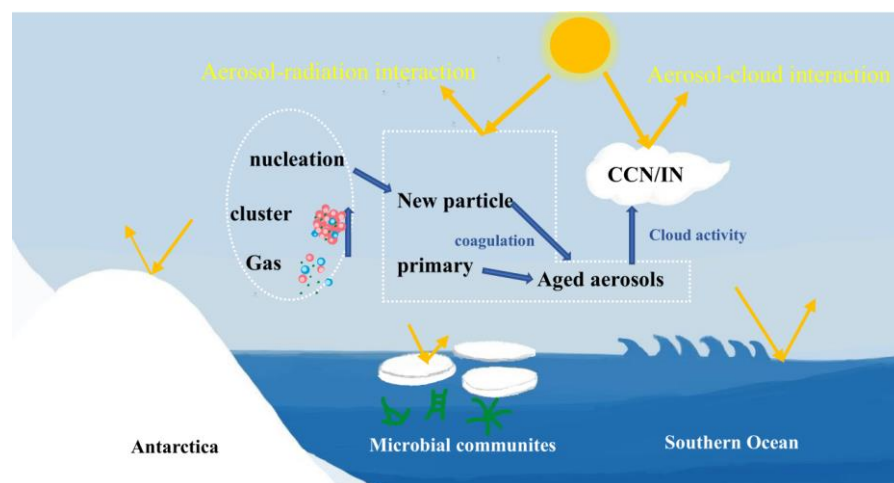


Figure 2. New particle formation over the SO and Antarctica and their effects on radiation.

There is a feedback loop involving the interaction among particle nucleation, CCN generation, cloud microphysics and climate response. Through a physics-based nucleation mechanism and a range of field observations of aerosol formation, it is shown that projected increases in global temperatures could significantly inhibit new particle and CCN formation rates worldwide. The reduction in CCN usually increases the average size of cloud droplets, reduces cloud albedo, increases precipitation, and reduces cloud cover. These lead to a reduced aerosol indirect radiative cooling effect of clouds that form on the CCN, thus amplifying the initial warming. Under actual conditions, the effect of temperature on CCN concentrations is likely to be more non-linear and the estimated 1–3% CCN decrease for each degree. The feedback process might contribute an additional forcing of $0.1\text{--}0.3 \text{ W m}^{-2}$

per degree of global warming, enough to increase the sensitivity of Earth's climate system significantly [82].

In addition, air masses during NPF events frequently originated from sea ice regions in the coastal Antarctica [61]. Thus, in the background of global warming, the influence of sea ice changes on NPF also deserves attention. Polar environments are significantly impacted by human-induced climate change and are warming twice as fast as the global average [29]. The changes in Antarctic climate and sea ice cover are complex. Between 1979 and 2014, the Antarctic sea ice extent actually slightly increased, and then it experienced a precipitous drop to below 1979 levels between 2015 and 2017. Antarctic sea ice is predicted to decrease by about 1/3 in response to greenhouse-gas-induced warming by the year 2100 [83,84]. Sea ice retreat in the polar region is expected to increase the emissions of sea salt aerosols and biogenic gases, which may significantly impact the climate by increasing CCN population and changing solar radiation [84]. In general, aerosol particle nucleation affects climate through aerosol–cloud interactions, while climate change affects particle nucleation process directly through global warming, or indirectly through sea ice variations [1,5,34,84]. More observations and model simulation research on the feedback mechanism between new particle formation and climate change are urgently needed.

Author Contributions: Conceptualization, methodology, funding acquisition, supervision, project administration, G.X. and L.C.; data curation, software, K.C.; writing original draft preparation, J.W. All authors have read and agreed to the published version of the manuscript.

Funding: The authors gratefully acknowledge the National Natural Science Foundation of China (Grant nos. 42006190); the open fund by the Key Laboratory of Global Change and Marine-Atmospheric Chemistry, Ministry of Natural Resources (MNR) (Grant nos. GCMAC1811); the Chinese Projects for Investigations and Assessments of the Arctic and Antarctic (Grant nos. CHINARE2010-2020) and Chinese International Cooperation Projects (Grant nos. 2009DFA22920) from the Ministry of Science and Technology (MOST).

Institutional Review Board Statement: Not applicable.

Informed Consent Statement: Not applicable.

Data Availability Statement: Not applicable.

Acknowledgments: We appreciate the great help from all crews of the R/V *Xuelong* during the Chinese National Antarctic Research Expeditions. The authors thank the Chinese Arctic and Antarctic Administration (CAA) and the Third Institute of Oceanography (TIO) of MNR for their support.

Conflicts of Interest: The authors declare no conflict of interest.

References

1. Lim, S.; Lee, M.; Rhee, T.S. Chemical characteristics of submicron aerosols observed at the King Sejong Station in the northern Antarctic Peninsula from fall to spring. *Sci. Total Environ.* **2019**, *668*, 1310–1316. [[CrossRef](#)] [[PubMed](#)]
2. Kyrö, E.M.; Kerminen, V.M.; Virkkula, A.; Dal Maso, M.; Parshintsev, J.; Ruíz-Jimenez, J.; Forsström, L.; Manninen, H.E.; Riekkola, M.L.; Heinonen, P.; et al. Antarctic new particle formation from continental biogenic precursors. *Atmos. Chem. Phys.* **2013**, *13*, 3527–3546. [[CrossRef](#)]
3. Kim, J.; Yoon, Y.J.; Gim, Y.; Choi, J.H.; Kang, H.J.; Park, K.-T.; Park, J.; Lee, B.Y. New particle formation events observed at King Sejong Station, Antarctic Peninsula—Part 1: Physical characteristics and contribution to cloud condensation nuclei. *Atmos. Chem. Phys.* **2019**, *19*, 7583–7594. [[CrossRef](#)]
4. Hara, K.; Nishita-Hara, C.; Osada, K.; Yabuki, M.; Yamanouchi, T. Characterization of aerosol number size distributions and their effect on cloud properties at Syowa Station, Antarctica. *Atmos. Chem. Phys.* **2021**, *21*, 12155–12172. [[CrossRef](#)]
5. Teinilä, K.; Frey, A.; Hillamo, R.; Tülp, H.C.; Weller, R. A study of the sea-salt chemistry using size-segregated aerosol measurements at coastal Antarctic station Neumayer. *Atmos. Environ.* **2014**, *96*, 11–19. [[CrossRef](#)]
6. Kammer, J.; Perraudin, E.; Flaud, P.M.; Lamaud, E.; Bonnefond, J.M.; Villenave, E. Observation of nighttime new particle formation over the French Landes forest. *Sci. Total Environ.* **2018**, *621*, 1084–1092. [[CrossRef](#)]
7. Charron, A.; Birmili, W.; Harrison, R.M. Factors influencing new particle formation at the rural site, Harwell, United Kingdom. *J. Geophys. Res.* **2007**, *112*, D14210. [[CrossRef](#)]

8. Hong, J.; Tang, M.; Wang, Q.; Ma, N.; Zhu, S.; Zhang, S.; Pan, X.; Xie, L.; Li, G.; Kuhn, U.; et al. Measurement Report: Wintertime new particle formation in the rural area of North China Plain: Influencing factors and possible formation mechanism. *Atmos. Chem. Phys. Discuss.* **2022**, *2022*, 1–32. [[CrossRef](#)]
9. Qiao, X.; Yan, C.; Li, X.; Guo, Y.; Yin, R.; Deng, C.; Li, C.; Nie, W.; Wang, M.; Cai, R.; et al. Contribution of Atmospheric Oxygenated Organic Compounds to Particle Growth in an Urban Environment. *Environ. Sci. Technol.* **2021**, *55*, 13646–13656. [[CrossRef](#)]
10. Bousiotis, D.; Pope, F.D.; Beddows, D.C.S.; Dall'Osto, M.; Massling, A.; Nøjgaard, J.K.; Nordstrøm, C.; Niemi, J.V.; Portin, H.; Petäjä, T.; et al. A phenomenology of new particle formation (NPF) at 13 European sites. *Atmos. Chem. Phys.* **2021**, *21*, 11905–11925. [[CrossRef](#)]
11. Zheng, G.; Wang, Y.; Wood, R.; Jensen, M.P.; Kuang, C.; McCoy, I.L.; Matthews, A.; Mei, F.; Tomlinson, J.M.; Shilling, J.E.; et al. New particle formation in the remote marine boundary layer. *Nat. Commun.* **2021**, *12*, 527. [[CrossRef](#)]
12. Huang, R.J.; Hoffmann, T.; Ovadnevaite, J.; Laaksonen, A.; Kokkola, H.; Xu, W.; Xu, W.; Ceburnis, D.; Zhang, R.; Seinfeld, J.H.; et al. Heterogeneous iodine-organic chemistry fast-tracks marine new particle formation. *Proc. Natl. Acad. Sci. USA* **2022**, *119*, e2201729119. [[CrossRef](#)]
13. Lachlan-Cope, T.; Beddows, D.C.S.; Brough, N.; Jones, A.E.; Harrison, R.M.; Lupi, A.; Yoon, Y.J.; Virkkula, A.; Dall'Osto, M. On the annual variability of Antarctic aerosol size distributions at Halley Research Station. *Atmos. Chem. Phys.* **2020**, *20*, 4461–4476. [[CrossRef](#)]
14. Herenz, P.; Wex, H.; Mangold, A.; Laffineur, Q.; Gorodetskaya, I.V.; Fleming, Z.L.; Panagi, M.; Stratmann, F. CCN measurements at the Princess Elisabeth Antarctica research station during three austral summers. *Atmos. Chem. Phys.* **2019**, *19*, 275–294. [[CrossRef](#)]
15. Alroe, J.; Cravigan, L.T.; Miljevic, B.; Johnson, G.R.; Selleck, P.; Humphries, R.S.; Keywood, M.D.; Chambers, S.D.; Williams, A.G.; Ristovski, Z.D. Marine productivity and synoptic meteorology drive summer-time variability in Southern Ocean aerosols. *Atmos. Chem. Phys.* **2020**, *20*, 8047–8062. [[CrossRef](#)]
16. Saliba, G.; Sanchez, K.J.; Russell, L.M.; Twohy, C.H.; Roberts, G.C.; Lewis, S.; Dedrick, J.; McCluskey, C.S.; Moore, K.; DeMott, P.J.; et al. Organic composition of three different size ranges of aerosol particles over the Southern Ocean. *Aerosol Sci. Technol.* **2020**, *55*, 268–288. [[CrossRef](#)]
17. O'Dowd, C.D.; Jimenez, J.L.; Bahreini, R.; Flagan, R.C.; Seinfeld, J.H.; Hämeri, K.; Pirjola, L.; Kulmala, M.; Jennings, S.G.; Hoffmann, T. Marine aerosol formation from biogenic iodine emissions. *Nature* **2002**, *417*, 632–636. [[CrossRef](#)]
18. Koponen, I.K.; Virkkula, A.; Hillamo, R.; Kerminen, V.M.; Kulmala, M. Number size distributions and concentrations of marine aerosols: Observations during a cruise between the English Channel and the coast of Antarctica. *J. Geophys. Res.* **2002**, *107*, D24. [[CrossRef](#)]
19. Cai, M.; Liang, B.; Sun, Q.; Liu, L.; Yuan, B.; Shao, M.; Huang, S.; Peng, Y.; Wang, Z.; Tan, H.; et al. The important roles of surface tension and growth rate in the contribution of new particle formation (NPF) to cloud condensation nuclei (CCN) number concentration: Evidence from field measurements in southern China. *Atmos. Chem. Phys.* **2021**, *21*, 8575–8592. [[CrossRef](#)]
20. Wang, J.; Li, M.; Li, L.; Zheng, R.; Fan, X.; Hong, Y.; Xu, L.; Chen, J.; Hu, B. Particle number size distribution and new particle formation in Xiamen, the coastal city of Southeast China in wintertime. *Sci. Total Environ.* **2022**, *826*, 154208. [[CrossRef](#)]
21. Holmes, N.S. A review of particle formation events and growth in the atmosphere in the various environments and discussion of mechanistic implications. *Atmos. Environ.* **2007**, *41*, 2183–2201. [[CrossRef](#)]
22. Lee, S.H.; Gordon, H.; Yu, H.; Lehtipalo, K.; Haley, R.; Li, Y.; Zhang, R. New Particle Formation in the Atmosphere: From Molecular Clusters to Global Climate. *J. Geophys. Res.* **2019**, *124*, 7098–7146. [[CrossRef](#)]
23. Kulmala, M.; Petäjä, T.; Nieminen, T.; Sipilä, M.; Manninen, H.E.; Lehtipalo, K.; Dal Maso, M.; Aalto, P.P.; Junninen, H.; Paasonen, P.; et al. Measurement of the nucleation of atmospheric aerosol particles. *Nat. Protoc.* **2012**, *7*, 1651–1667. [[CrossRef](#)]
24. Wang, Z.; Hu, M.; Wu, Z.; Yue, D. Research on the Formation Mechanisms of New Particles in the Atmosphere. *Acta Chim. Sin.* **2013**, *71*, 519–527. (In Chinese) [[CrossRef](#)]
25. Vu, T.V.; Delgado-Saborit, J.M.; Harrison, R.M. Review: Particle number size distributions from seven major sources and implications for source apportionment studies. *Atmos. Environ.* **2015**, *122*, 114–132. [[CrossRef](#)]
26. Su, P.; Joutsensaari, J.; Dada, L.; Zaidan, M.A.; Nieminen, T.; Li, X.; Wu, Y.; Decesari, S.; Tarkoma, S.; Petäjä, T.; et al. New particle formation event detection with Mask R-CNN. *Atmos. Chem. Phys.* **2022**, *22*, 1293–1309. [[CrossRef](#)]
27. Kulmala, M.; Kerminen, V.-M. On the formation and growth of atmospheric nanoparticles. *Atmos. Res.* **2008**, *90*, 132–150. [[CrossRef](#)]
28. Brean, J.; Dall'Osto, M.; Simó, R.; Shi, Z.; Beddows, D.C.S.; Harrison, R.M. Open ocean and coastal new particle formation from sulfuric acid and amines around the Antarctic Peninsula. *Nat. Geosci.* **2021**, *14*, 383–388. [[CrossRef](#)]
29. Quéléver, L.L.J.; Dada, L.; Asmi, E.; Lampilahti, J.; Chan, T.; Ferrara, J.E.; Copes, G.E.; Pérez-Fogwill, G.; Barreira, L.; Aurela, M.; et al. Investigation of new particle formation mechanisms and aerosol processes at Marambio Station, Antarctic Peninsula. *Atmos. Chem. Phys.* **2022**, *22*, 8417–8437. [[CrossRef](#)]
30. Arquero, K.D.; Gerber, R.B.; Finlayson-Pitts, B.J. The Role of Oxalic Acid in New Particle Formation from Methanesulfonic Acid, Methylamine, and Water. *Environ. Sci. Technol.* **2017**, *51*, 2124–2130. [[CrossRef](#)]
31. Yu, S. Role of organic acids (formic, acetic, pyruvic and oxalic) in the formation of cloud condensation nuclei (CCN): A review. *Atmos. Res.* **2000**, *53*, 185–217. [[CrossRef](#)]

32. Sipilä, M.; Sarnela, N.; Neitola, K.; Laitinen, T.; Kemppainen, D.; Beck, L.; Duplissy, E.-M.; Kuittinen, S.; Lehmusjärvi, T.; Lampilahti, J.; et al. Wintertime subarctic new particle formation from Kola Peninsula sulfur emissions. *Atmos. Chem. Phys.* **2021**, *21*, 17559–17576. [[CrossRef](#)]
33. Kulmala, M.; Laaksonen, A. Binary nucleation of water–sulfuric acid system: Comparison of classical theories with different H₂SO₄ saturation vapor pressures. *J. Chem. Phys.* **1990**, *93*, 696–701. [[CrossRef](#)]
34. Korhonen, P.; Kulmala, M.; Laaksonen, A.; Viisanen, Y.; McGraw, R.; Seinfeld, J.H. Ternary nucleation of H₂SO₄, NH₃, and H₂O in the atmosphere. *J. Geophys. Res.* **1999**, *104*, 26349–26353. [[CrossRef](#)]
35. Yu, F.; Luo, G.; Nair, A.A.; Eastham, S.; Williamson, C.J.; Kupc, A.; Brock, C.A. Particle number concentrations and size distributions in the stratosphere: Implications of nucleation mechanisms and particle microphysics. *Atmos. Chem. Phys.* **2023**, *23*, 1863–1877. [[CrossRef](#)]
36. Yu, F.; Luo, G. Simulation of particle size distribution with a global aerosol model: Contribution of nucleation to aerosol and CCN number concentrations. *Atmos. Chem. Phys.* **2009**, *9*, 7691–7710. [[CrossRef](#)]
37. Sipilä, M.; Lehtipalo, K.; Kulmala, M. Atmospheric Particle Nucleation. *Aerosol Sci.* **2013**, *7*, 153–180. [[CrossRef](#)]
38. Spracklen, D.V.; Carslaw, K.S.; Kulmala, M.; Kerminen, V.M.; Mann, G.W.; Sihto, S.L. The contribution of boundary layer nucleation events to total particle concentrations on regional and global scales. *Atmos. Chem. Phys.* **2006**, *6*, 5631–5648. [[CrossRef](#)]
39. Yu, F.; Luo, G.; Bates, T.S.; Anderson, B.; Clarke, A.; Kapustin, V.; Yantosca, R.M.; Wang, Y.; Wu, S. Spatial distributions of particle number concentrations in the global troposphere: Simulations, observations, and implications for nucleation mechanisms. *J. Geophys. Res.* **2010**, *115*, D17205. [[CrossRef](#)]
40. Yao, L.; Garmash, O.; Bianchi, F.; Zheng, J.; Yan, C.; Kontkanen, J.; Junninen, H.; Mazon, S.B.; Ehn, M.; Paasonen, P.; et al. Atmospheric new particle formation from sulfuric acid and amines in a Chinese megacity. *Science* **2018**, *361*, 278–281. [[CrossRef](#)]
41. Ning, A.; Liu, L.; Ji, L.; Zhang, X. Molecular-level nucleation mechanism of iodic acid and methanesulfonic acid. *Atmos. Chem. Phys.* **2022**, *22*, 6103–6114. [[CrossRef](#)]
42. Ramachandran, G.; Park, J.Y.; Raynor, P.C. *Assessing Exposures to Nanomaterials in the Occupational Environment*; Elsevier: Amsterdam, The Netherlands, 2011.
43. Kangasluoma, J.; Ahonen, L.R.; Laurila, T.M.; Cai, R.; Enroth, J.; Mazon, S.B.; Korhonen, F.; Aalto, P.P.; Kulmala, M.; Attoui, M.; et al. Laboratory verification of a new high flow differential mobility particle sizer, and field measurements in Hyytiälä. *J. Aerosol Sci.* **2018**, *124*, 1–9. [[CrossRef](#)]
44. Volckens, J.; Peters, T.M. Counting and particle transmission efficiency of the aerodynamic particle sizer. *J. Aerosol Sci.* **2005**, *36*, 1400–1408. [[CrossRef](#)]
45. Zhang, J.; Chen, D. Differential Mobility Particle Sizers for Nanoparticle Characterization. *J. Nanotechnol. Eng. Med.* **2014**, *5*, 9. [[CrossRef](#)]
46. Seifert, M.; Tiede, R.; Schnaiter, M.; Linke, C.; Möhler, O.; Schurath, U.; Ström, J. Operation and performance of a differential mobility particle sizer and a TSI 3010 condensation particle counter at stratospheric temperatures and pressures. *J. Aerosol Sci.* **2004**, *35*, 981–993. [[CrossRef](#)]
47. North, G.R.; Pyle, J.A.; Zhang, F. (Eds.) *Encyclopedia of Atmospheric Sciences*; Elsevier: Amsterdam, The Netherlands, 2014; Volume 1.
48. Loizidis, C.; Costi, M.; Lekaki, N.; Bezantakos, S.; Biskos, G. Improved performance of Differential Mobility Analyzers with 3D-printed flow straighteners. *J. Aerosol Sci.* **2020**, *145*, 105545. [[CrossRef](#)]
49. Belosi, F.; Contini, D.; Donato, A.; Santachiara, G.; Prodi, F. Aerosol size distribution at Nansen Ice Sheet Antarctica. *Atmos. Res.* **2012**, *107*, 42–50. [[CrossRef](#)]
50. Lewis, A.; Edwards, P. Validate personal air-pol sensors lution. *Nature* **2016**, *535*, 29–31. [[CrossRef](#)]
51. Schmale, J.; Baccarini, A.; Thurnherr, I.; Henning, S.; Efraim, A.; Regayre, L.; Bolas, C.; Hartmann, M.; Welti, A.; Lehtipalo, K.; et al. Overview of the Antarctic Circumnavigation Expedition: Study of Preindustrial-like Aerosols and Their Climate Effects (ACE-SPACE). *Bull. Am. Meteorol. Soc.* **2019**, *100*, 2260–2283. [[CrossRef](#)]
52. Koponen, I.K.; Virkkula, A.; Hillamo, R.; Kerminen, V.-M.; Kulmala, M. Number size distributions and concentrations of the continental summer aerosols in Queen Maud Land, Antarctica. *J. Geophys. Res.* **2003**, *108*, D18. [[CrossRef](#)]
53. Weller, R.; Legrand, M.; Preunkert, S. Size distribution and ionic composition of marine summer aerosol at the continental Antarctic site Kohnen. *Atmos. Chem. Phys.* **2018**, *18*, 2413–2430. [[CrossRef](#)]
54. Järvinen, E.; Virkkula, A.; Nieminen, T.; Aalto, P.P.; Asmi, E.; Lanconelli, C.; Busetto, M.; Lupi, A.; Schioppo, R.; Vitale, V.; et al. Seasonal cycle and modal structure of particle number size distribution at Dome C, Antarctica. *Atmos. Chem. Phys.* **2013**, *13*, 7473–7487. [[CrossRef](#)]
55. Hara, K.; Osada, K.; Nishita-Hara, C.; Yamanouchi, T. Seasonal variations and vertical features of aerosol particles in the Antarctic troposphere. *Atmos. Chem. Phys.* **2011**, *11*, 5471–5484. [[CrossRef](#)]
56. Revell, L.E.; Kremser, S.; Hartery, S.; Harvey, M.; Mulcahy, J.P.; Williams, J.; Morgenstern, O.; McDonald, A.J.; Varma, V.; Bird, L.; et al. The sensitivity of Southern Ocean aerosols and cloud microphysics to sea spray and sulfate aerosol production in the HadGEM3-GA7.1 chemistry–climate model. *Atmos. Chem. Phys.* **2019**, *19*, 15447–15466. [[CrossRef](#)]
57. Yu, F.; Luo, G. Oceanic Dimethyl Sulfide Emission and New Particle Formation around the Coast of Antarctica: A Modeling Study of Seasonal Variations and Comparison with Measurements. *Atmosphere* **2010**, *1*, 34–50. [[CrossRef](#)]

58. Jokinen, T.; Sipilä, M.; Kontkanen, J.; Vakkari, V.; Tisler, P.; Duplissy, E.M.; Junninen, H.; Kangasluoma, J.; Manninen, H.E.; Petäjä, T.; et al. Ion-induced sulfuric acid-ammonia nucleation drives particle formation in coastal Antarctica. *Sci. Adv.* **2018**, *4*, eaat9744. [[CrossRef](#)]
59. Burrell, E.; Kar, T.; Hansen, J.C. Computational Study of the Thermodynamics of New Particle Formation Initiated by Complexes of $\text{H}_2\text{SO}_4\text{-H}_2\text{O-NH}_x$, $\text{CH}_3\text{SO}_3\text{H-H}_2\text{O-NH}_x$, and $\text{HO}_2\text{-H}_2\text{O-NH}_x$. *ACS Earth Space Chem.* **2019**, *3*, 1415–1425. [[CrossRef](#)]
60. Lana, A.; Bell, T.G.; Simó, R.; Vallina, S.M.; Ballabrera-Poy, J.; Kettle, A.J.; Dachs, J.; Bopp, L.; Saltzman, E.S.; Stefels, J.; et al. An updated climatology of surface dimethylsulfide concentrations and emission fluxes in the global ocean. *Glob. Biogeochem. Cycles* **2011**, *25*, GB1004. [[CrossRef](#)]
61. Baccarini, A.; Dommen, J.; Lehtipalo, K.; Henning, S.; Modini, R.L.; Gysel-Beer, M.; Baltensperger, U.; Schmale, J. Low-Volatility Vapors and New Particle Formation Over the Southern Ocean During the Antarctic Circumnavigation Expedition. *J. Geophys. Res.* **2021**, *126*, e2021JD035126. [[CrossRef](#)]
62. Hirsikko, A.; Nieminen, T.; Gagné, S.; Lehtipalo, K.; Manninen, H.E.; Ehn, M.; Hörrak, U.; Kerminen, V.M.; Laakso, L.; McMurry, P.H.; et al. Atmospheric ions and nucleation: A review of observations. *Atmos. Chem. Phys.* **2011**, *11*, 767–798. [[CrossRef](#)]
63. Stolzenburg, D.; Simon, M.; Ranjithkumar, A.; Kürten, A.; Lehtipalo, K.; Gordon, H.; Ehrhart, S.; Finkenzeller, H.; Pichelstorfer, L.; Nieminen, T.; et al. Enhanced growth rate of atmospheric particles from sulfuric acid. *Atmos. Chem. Phys.* **2020**, *20*, 7359–7372. [[CrossRef](#)]
64. Zhang, R.; Khalizov, A.; Wang, L.; Hu, M.; Xu, W. Nucleation and growth of nanoparticles in the atmosphere. *Chem. Rev.* **2012**, *112*, 1957–2011. [[CrossRef](#)]
65. Peltola, M.; Rose, C.; Trueblood, J.V.; Gray, S.; Harvey, M.; Sellegri, K. New particle formation in coastal New Zealand with a focus on open-ocean air masses. *Atmos. Chem. Phys.* **2022**, *22*, 6231–6254. [[CrossRef](#)]
66. He, X.C.; Tham, Y.J.; Dada, L.; Wang, M.; Finkenzeller, H.; Stolzenburg, D.; Iyer, S.; Simon, M.; Kürten, A.; Shen, J.; et al. Role of iodine oxoacids in atmospheric aerosol nucleation. *Science* **2021**, *371*, 589–595. [[CrossRef](#)]
67. Roscoe, H.K.; Jones, A.E.; Brough, N.; Weller, R.; Saiz-Lopez, A.; Mahajan, A.S.; Schoenhardt, A.; Burrows, J.P.; Fleming, Z.L. Particles and iodine compounds in coastal Antarctica. *J. Geophys. Res.* **2015**, *120*, 7144–7156. [[CrossRef](#)]
68. Ning, A.; Liu, L.; Zhang, S.; Yu, F.; Du, L.; Ge, M.; Zhang, X. The critical role of dimethylamine in the rapid formation of iodic acid particles in marine areas. *npj Clim. Atmos. Sci.* **2022**, *5*, 92. [[CrossRef](#)]
69. Sipilä, M.; Sarnela, N.; Jokinen, T.; Henschel, H.; Junninen, H.; Kontkanen, J.; Richters, S.; Kangasluoma, J.; Franchin, A.; Peräkylä, O.; et al. Molecular-scale evidence of aerosol particle formation via sequential addition of HIO_3 . *Nature* **2016**, *537*, 532–534. [[CrossRef](#)]
70. Wang, S.; Yan, J.; Lin, Q.; Zhang, M.; Xu, S.; Zhao, S.; Ruan, M. Formation of marine secondary aerosols in the Southern Ocean, Antarctica. *Environ. Chem.* **2021**, *18*, 285–293. [[CrossRef](#)]
71. Humphries, R.S.; Schofield, R.; Keywood, M.D.; Ward, J.; Pierce, J.R.; Gionfriddo, C.M.; Tate, M.T.; Krabbenhoft, D.P.; Galbally, I.E.; Molloy, S.B.; et al. Boundary layer new particle formation over East Antarctic sea ice—Possible Hg-driven nucleation? *Atmos. Chem. Phys.* **2015**, *15*, 13339–13364. [[CrossRef](#)]
72. Yue, F.; Xie, Z.; Yan, J.; Zhang, Y.; Jiang, B. Spatial Distribution of Atmospheric Mercury Species in the Southern Ocean. *J. Geophys. Res.* **2021**, *126*, e2021JD034651. [[CrossRef](#)]
73. Kerminen, V.-M.; Chen, X.; Vakkari, V.; Petäjä, T.; Kulmala, M.; Bianchi, F. Atmospheric new particle formation and growth: Review of field observations. *Environ. Res. Lett.* **2018**, *13*, 103003. [[CrossRef](#)]
74. Chen, X.; Yu, F.; Yang, W.; Sun, Y.; Chen, H.; Du, W.; Zhao, J.; Wei, Y.; Wei, L.; Du, H.; et al. Global–regional nested simulation of particle number concentration by combining microphysical processes with an evolving organic aerosol module. *Atmos. Chem. Phys.* **2021**, *21*, 9343–9366. [[CrossRef](#)]
75. Shirsat, S.V.; Graf, H.F. An emission inventory of sulfur from anthropogenic sources in Antarctica. *Atmos. Chem. Phys.* **2009**, *9*, 3397–3408. [[CrossRef](#)]
76. Twohy, C.H.; DeMott, P.J.; Russell, L.M.; Toohey, D.W.; Rainwater, B.; Geiss, R.; Sanchez, K.J.; Lewis, S.; Roberts, G.C.; Humphries, R.S.; et al. Cloud-Nucleating Particles Over the Southern Ocean in a Changing Climate. *Earth's Future* **2021**, *9*, e2020EF001673. [[CrossRef](#)]
77. Pierce, J.R.; Adams, P.J. Efficiency of cloud condensation nuclei formation from ultrafine particles. *Atmos. Chem. Phys.* **2007**, *7*, 1367–1379. [[CrossRef](#)]
78. Merikanto, J.; Spracklen, D.V.; Mann, G.W.; Pickering, S.J.; Carslaw, K.S. Impact of nucleation on global CCN. *Atmos. Chem. Phys.* **2009**, *9*, 8601–8616. [[CrossRef](#)]
79. McCoy, I.L.; Bretherton, C.S.; Wood, R.; Twohy, C.H.; Gettelman, A.; Bardeen, C.G.; Toohey, D.W. Influences of Recent Particle Formation on Southern Ocean Aerosol Variability and Low Cloud Properties. *J. Geophys. Res.* **2021**, *126*, e2020JD033529. [[CrossRef](#)]
80. Salim, S.N.; Adhikari, A.; Shaikh, A.A.; Menon, H.B.; Kumar, N.; Rajeev, K. Aerosol-boundary layer dynamics and its effect on aerosol radiative forcing and atmospheric heating rate in the Indian Ocean sector of Southern Ocean. *Sci. Total Environ.* **2023**, *858*, 159770. [[CrossRef](#)]
81. Angeles Suazo, J.M.; Suarez Salas, L.; Huaman De La Cruz, A.R.; Angeles Vasquez, R.; Rosales Aylas, G.; Rocha Condor, A.; Requena Rojas, E.; Muñoz Ccuro, F.; Flores Rojas, J.L.; Abi Karam, H. Direct Radiative Forcing Due to Aerosol Properties at the Peruvian Antarctic Station and Metropolitan Huancayo Area. *Anuário. do Instituto de Geociências* **2020**, *43*, 404–412. [[CrossRef](#)]

82. Yu, F.; Luo, G.; Turco, R.P.; Ogren, J.A.; Yantosca, R.M. Decreasing particle number concentrations in a warming atmosphere and implications. *Atmos. Chem. Phys.* **2012**, *12*, 2399–2408. [[CrossRef](#)]
83. Bracegirdle, T.J.; Connolley, W.M.; Turner, J. Antarctic climate change over the twenty first century. *J. Geophys. Res.* **2008**, *113*, D03103. [[CrossRef](#)]
84. Yan, J.; Jung, J.; Lin, Q.; Zhang, M.; Xu, S.; Zhao, S. Effect of sea ice retreat on marine aerosol emissions in the Southern Ocean, Antarctica. *Sci. Total Environ.* **2020**, *745*, 140773. [[CrossRef](#)]

Disclaimer/Publisher’s Note: The statements, opinions and data contained in all publications are solely those of the individual author(s) and contributor(s) and not of MDPI and/or the editor(s). MDPI and/or the editor(s) disclaim responsibility for any injury to people or property resulting from any ideas, methods, instructions or products referred to in the content.